

Explainable Censored Learning: Finding Critical Features with Long Term Prognostic Values for Survival Prediction

Xinxing Wu^a, Chong Peng^b, Richard Charnigo^c, and Qiang Cheng^{a,1}

^a*Institute for Biomedical Informatics, University of Kentucky, Lexington, KY 40506, USA*

^b*Department of Computer Science and Engineering, Qingdao University, Shandong 266071, China*

^c*Department of Statistics, University of Kentucky, Lexington, KY 40536, USA*

Abstract

Interpreting critical variables involved in complex biological processes related to survival time can help understand prediction from survival models, evaluate treatment efficacy, and develop new therapies for patients. Currently, the predictive results of deep learning (DL)-based models are better than or as good as standard survival methods, they are often disregarded because of their lack of transparency and little interpretability, which is crucial to their adoption in clinical applications. In this paper, we introduce a novel, easily deployable approach, called EXplainable CEnsored Learning (EXCEL), to iteratively exploit critical variables and simultaneously implement (DL) model training based on these variables. First, on a toy dataset, we illustrate the principle of EXCEL; then, we mathematically analyze our proposed method, and we derive and prove tight generalization error bounds; next, on two semi-synthetic datasets, we show that EXCEL has good anti-noise ability and stability; finally, we apply EXCEL to a variety of real-world survival datasets including clinical data and genetic data, demonstrating that EXCEL can effectively identify critical features and achieve performance on par with or better than the original models. It is worth pointing out that EXCEL is flexibly deployed in existing or emerging models

¹Correspondence should be addressed to: qiang.cheng@uky.edu. Address: RM 230, Multidisciplinary Science Building, KY 40506, USA. Phone number: 859-323-7238.

for explainable survival data in the presence of right censoring.

Keywords: Censored Learning, deep learning, feature selection, generalization error bound

1. Introduction

Different from common prediction tasks in machine learning, survival analysis focuses on modeling censored data. The Cox proportional-hazards (CPH) model [1] is a standard regression model widely used in epidemiological studies and clinical trials, e.g., for analyzing gene expression- or clinical variable-related time-to-event survival data. Recently, deep learning (DL)-based techniques have been adapted for CPH, such as DeepSurv [2], Cox-nnet [3], and PASNet [4]. Although the predictive results of these DL-based models are better than or as good as standard survival methods, they are often disregarded because of their lack of transparency and little interpretability [5], which is crucial to their adoption in clinical applications. In survival analysis, an important goal is to identify potential risk factors from thousands of variables to evaluate treatment effects [7]. Kaplan-Meier (KM) curves [8] and Log-rank tests [9, 10] are two typical methods for univariate factor analysis, describing survival in terms of one factor but ignoring the impact of the other variables.² The CPH model, as a representative survival analysis method, can assess survival prediction based on risk variables. To identify informative variables in the CPH model, variable selection via penalization like employing an ℓ_0 -norm is statistically preferred and has attracted much attention in recent years. Because the exact ℓ_0 optimization needs to search the space of all possible subsets, which is an NP-hard problem [11, 12, 13], a variety of convex surrogate functions for ℓ_0 -norm have been developed. The Lasso [14, 15] penalty, i.e., ℓ_1 -norm regularization, is a popular

²KM estimation is a non-parametric method which uses data from subjects at one level of the univariate factor to construct a non-increasing step function which approximates the survival probability in relation to time. Log-rank test is a non-parametric method which uses data from independent subjects at different levels of the univariate factor to test a null hypothesis of identical survival probabilities in relation to time.

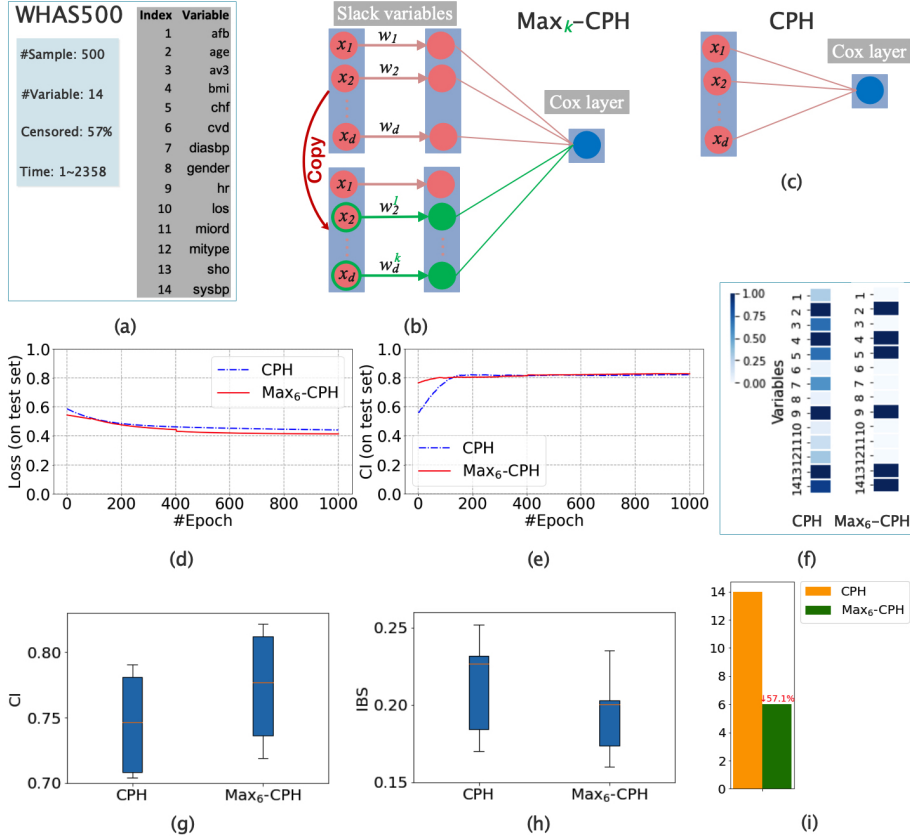


Figure 1: Schematic illustration of our EXCEL approach embedded in the standard CPH model (denoted as $\text{Max}_k\text{-CPH}$) and its comparison with the baseline model on dataset Worcester Heart Attack Study (WHAS500). (a) The statistic of dataset WHAS500. We directly import function `sksurv.datasets.load_whas500()` (for more details, see https://scikit-survival.readthedocs.io/en/latest/api/generated/sksurv.datasets.load_whas500.html) to download WHAS500 [6]; (b) and (c) are the architectures of $\text{Max}_k\text{-CPH}$ and the baseline, respectively; (d) and (e) are the loss and CI comparisons of $\text{Max}_k\text{-CPH}$ with the baseline model with different epochs on the test set; (f) The comparison of variable selection of our method with the baseline; (g)-(h) The performance comparison of our method with the baseline model in CI and IBS with 5 random training/test set splits; (i) The comparison of the number of used variables of our method with the baseline.

one; however, [16] pointed out that convex surrogate functions, such as ℓ_1 -norm, generally bring non-negligible estimation biases and thus an adverse effect on the predictive ability. Lately, [17] used two convex programs to optimize the CPH model with a non-convex penalty for variable selection; [18] generalized the primal-dual active set algorithm for general convex loss functions to solve the best subset constraint problem, such as the sparse CPH model with an ℓ_0 -norm-based constraint, and developed the corresponding R package, `BeSS`. Although these existing works can select useful variables in the baseline CPH model, effective ways to identify critical factors in DL-based survival analysis is evasive; in particular, due to their being generally non-convex, it is impossible to directly apply these existing techniques for the CPH model to the DL-based models.

In this paper, we aim to find critical features with long-term prognostic values and help establish necessary explainability for the prognosis of survival time in DL-based survival analysis over censored data. To overcome the bias issue of the ℓ_1 -norm based sparse CPH model, we develop an approach for DL-based survival models by leveraging a direct counterpart of the ℓ_0 -norm regularization. Inspired by the recent development of feature selection algorithms in unsupervised learning [19, 20], we adopt an ℓ_1 -norm regularization to score all input variables globally, and then determine the k variables with the maximum scores as a counterpart of ℓ_0 norm, to iteratively revamp the learning of our target model. We dub this approach EXplainable CEnsored Learning (EXCEL). Notably, EXCEL has a high stability advantage in that its identified factors do not change much with different subsets of training examples, in sharp contrast to other methods; see Figure 3 (k). The schematic of EXCEL is illustrated in Figure 1 with a toy dataset, WHAS500. The EXCEL-extended CPH model for selecting k features, denoted by Max_k -CPH, is shown in Figure 1 (b). Compared to the standard CPH model shown in Figure 1 (c), our proposed method has one more layer of slack variables and a Max_k embedded module (marked in green) as our target model. The slack variables are used to score the importance of all input survival variables globally, while the Max_k module implements learning

based on k selected variables with the maximum scores in each iteration. Figure 1 (d) and (e) show that, on the test set of WHAS500 with $k = 6$, with the increase of epoch, our method achieves a smaller loss and better concordance index (CI) than the standard CPH model. Figure 1 (f) and (g) indicate that our method performs better in CI and integrated Brier score (IBS) than the standard CPH model with 5 random training/test set splits. Figure 1 (h) shows that our model uses 57.1% fewer variables than the standard CPH model.

Technically, our designed algorithm trains a (DL-based) survival model to identify potentially informative variables for survival learning globally; simultaneously, it leverages an embedded module to select a subset locally from the globally informative variables to examine their diversity, which is efficiently measured by their abilities to fit the survival time. In this way, the embedded module enables us to effectively screen out the critical variables for predicting the survival time. The global component turns out to play a crucial role in regularization to stabilize the variable selecting process, similar to [19]. By capitalizing on such a regularization, we find that the resulting embedded model can select representative variables and simultaneously capture the complex non-linear relationship between these variables and survival time. In Section **Algorithm development and analysis**, we derive and prove a tight generalization error bound for the difference between the solution of the lead model and that of the induced model, thereby providing theoretical certificates of using our proposed regularization for variable selection. Notably, our method can be deployed as a lightweight module, easily plugged in, and efficiently optimized along with the existing standard survival methods, including DeepSurv, Coxnet, and PASNet. In Section **Experimental results**, on two semi-synthetic datasets and three real-world survival datasets, including clinical and genetic data, with varying numbers of subjects and variables and portions of censored observations, we demonstrate that our proposed EXCEL approach can identify critically important risk factors from thousands of variables potentially related to the survival time and, with only a small subset of identified variables, it can achieve prognostic performance comparable to or better than the original

85 models with all variables.³

2. Algorithm development and analysis

Description of the algorithm. Set $[N] = \{1, 2, \dots, N\}$. Let $\mathcal{D} = \{x_i, E_i, T_i\}_{i=1}^N$ be a survival dataset consisting of N subjects, where $x_i \in \mathbb{R}^{d \times 1}, i \in [N]$; E_i is the censoring indicator: $E_i = 0$ if the survival time of subject i was (right) 90 censored, and $E_i = 1$ otherwise; T_i is the censored survival time for subject i as indicated by E_i . Usually, a maximum likelihood-based approach is adopted to model the distribution $S(t|x) = \mathbb{P}(T > t|x)$ from survival data [1]. And we assume all samples are bounded, i.e., $\forall x_i, i \in [N], \exists C_1 \geq 0$, such that $\sum_{i \in [N]} \|x_i\|_2 \leq C_1$.

Here, we use the average negative log partial likelihood function as the loss function, and we give a more general form as follows:

$$\mathcal{L}(f, \mathcal{D}) \triangleq -\frac{1}{N_{E=1}} \sum_{i: E_i=1} \left(f(x_i) - \log \sum_{T_j \geq T_i} \exp f(x_j) \right) + \lambda_1 \cdot \text{Reg}(f), \quad (1)$$

95 where $N_{E=1}$ is the number of patients of nonzero E (i.e., observable events), $f(\cdot)$ is a generally a non-convex function, e.g., a neural network, and $\text{Reg}(f)$ represents the regularizations on $f(\cdot)$. The above model is a generalization of a number of existing survival models: 1) It reduces to DeepSurv if f is parameterized as a neural network and $f \in \mathbb{R}$. 2) It reduces to Cox-nnet if 100 f can be written as $\beta^T g$, where g is a neural network, $g \in \mathbb{R}^{m \times 1}$, β denotes the weights in a standard CPH model that need to be trained, $\beta \in \mathbb{R}^{m \times 1}$, and m is an integer. 3) It becomes PASNet if the first layer of g can be further rewritten as $W_{g_1} \odot M$, where \odot denotes element-wise multiplication and the elements of M are either one or zero, determining which associated weights are dropped 105 during training. And $W_{g_1}, M \in \mathbb{R}^{d \times k_1}$, k_1 denotes the number of neurons in the

³For original models with all variables, we denote that the training of models directly uses all of the potentially variables of the sample, rather than a subset of variables of the input sample.

first layer of g .

Our proposed EXCEL approach introduces a sub-architecture to existing models and (1) becomes

$$\begin{aligned}
& \mathcal{L}(f, W_I, \mathcal{D}) \\
\triangleq & -\frac{\lambda_0}{N_{E=1}} \sum_{i: E_i=1} \left(f(W_I x_i) - \log \sum_{T_j \geq T_i} \exp f(W_I x_j) \right) \\
& -\frac{\lambda_2}{N_{E=1}} \sum_{i: E_i=1} \left(f(W_I^{\max_k} x_i) - \log \sum_{T_j \geq T_i} \exp f(W_I^{\max_k} x_j) \right) \\
& +\lambda_1 \cdot \text{Reg}(f) + \lambda_3 \cdot \text{Reg}(W_I),
\end{aligned} \tag{2}$$

where $W_I^{\max_k} = \text{Diag}(w^{\max_k}) (\in \mathbb{R}^{d \times d})$ and $w^{\max_k} (\in \mathbb{R}^{d \times 1})$ is an operation to keep the k largest entries of w while making other entries 0. We generally take $\text{Reg}(W_I)$ as $\|W_I\|_1$. In practical computation, we constrain the elements in W_I to be non-negative, to simplify the processing of variable scores; otherwise, during optimization, we need to take the absolute value of the scores first before performing Max_k operation.

The optimization of (3) is an efficient extension of the DL-based survival models of (1), where the main difference comes from the second term of (3). In each iteration of back propagation, the second term of (3) would require the gradients of the variables corresponding to the maximal k weights in magnitude during this iteration while not affecting the gradients of other variables. Note that the EXCEL-extended model in the second term essentially has the same architecture as the DL-based model, i.e., (1). Thus, the gradients of the second term can reuse (up to a multiplicative factor) those corresponding to the maximal k weights from the first term, with only an additional ranking operation. Finding the maximal k out of d weights in each iteration has a worst-case efficiency $\mathcal{O}(d \min\{\log d, k\})$ that is independent of N . Therefore, the efficiency of optimizing (3) is essentially the same as (1).

Notably, the EXCEL approach can be easily used for many existing survival models, and we illustrate the schematic of the EXCEL-extended models for

DeepSurv, Cox-nnet, and PASNet in Figure 2.

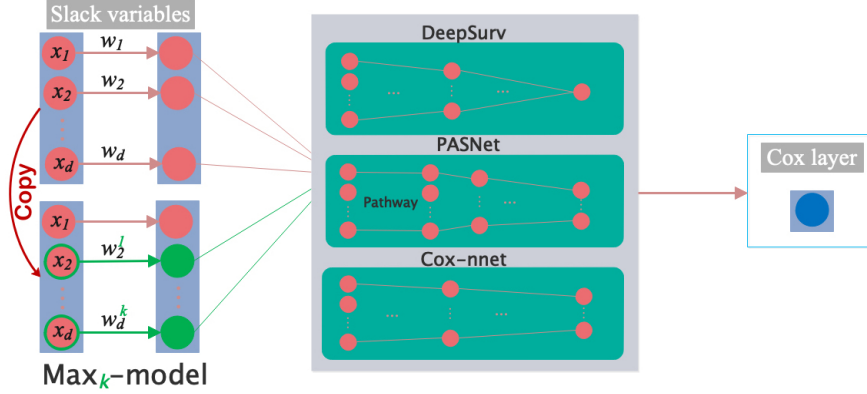


Figure 2: Schematic illustration of the EXCEL-extended models for various DL-based survival models.

Evaluation metrics. Two main metrics are adopted for evaluating the performance of survival models: 1) Concordance index (CI) [21, 22] is widely used to evaluate the ability of models to rank individuals by their risk for the time-to-event predictions. The larger the CI value, the better the performance. 2) Integrated Brier Score (IBS) [23] extends Brier score [24] to right-censored data for evaluating the accuracy of an estimated survival function at time t . The smaller the IBS value, the better the performance. In our experiments, we directly import function `sksurv.metrics.concordance_index_censored()` and `sksurv.metrics.integrated_brier_score()` for calculating CI and IBS.

Experimental setting. In our experiments, we set the maximum number of epochs to be 150 for two semi-synthetic datasets NSurvUSPS_3vs8 and SurvUSPS_3vs8 and 1,000 for real-world datasets, including WHAS500, Breast cancer, SUPPORT, and GBM. We initialize the weights of variable selection layer by sampling uniformly from $U[0.999999, 0.9999999]$ and the other layers with the Xavier normal initializer [25]. We adopt the Adam optimizer [26] with an initialized learning rate of 0.0001. For the hyper-parameter setting, we perform a grid search on the validation set, and then choose the optimal one. Taking (3) as an example, we mainly need to optimize four hyper-parameters. On the validation set split from training set, we optimize λ_0 and λ_2 over the search space:

[0.4, 0.8, 1.2, 1.6], and λ_1 and λ_3 over the search space: [0.0001, 0.0005, 0.001, 0.005, 0.01, 0.05, 0.1, 0.5].

For all datasets, we randomly split them into training and testing sets by
 150 a ratio of 80:20; the results are averaged over 10 runs of 10 different random
 splits for the results on the three datasets. All experiments are implemented
 with Python 3.7.8. The codes will be made publicly available upon acceptance.

Generalization error bounds. Now, we study the error bound for the difference between the solution of the lead model and that of the induced model. For analytical tractability, we focus on shallow neural networks (NNs) with the ℓ_2 -norm regularization here and our analysis may be extended to more general NNs with more layers and we will leave the extension as a line for future study. The optimization consists of minimizing the following average negative log partial likelihood objective function:

$$\begin{aligned} & \mathcal{L}(w, \mathcal{D}) \\ = & -\frac{1}{N_{E=1}} \sum_{i:E_i=1} \left(x_i^T w - \log \sum_{T_j \geq T_i} \exp(x_j^T w) \right) \\ & -\frac{\lambda_2}{N_{E=1}} \sum_{i:E_i=1} \left(x_i^T w^{\max_k} - \log \sum_{T_j \geq T_i} \exp(x_j^T w^{\max_k}) \right) + \frac{\lambda_3}{2} \|w\|_2^2. \end{aligned} \quad (3)$$

In practical computation, we constrain the elements in w to be non-negative, to simplify the processing of variable scores; otherwise, during optimization,
 155 we need to take the absolute value of the scores first before performing Max_k
 operation.

Let $\hat{w} = \arg \min_{w \in \mathbb{R}^{d \times 1}} \mathcal{L}(w, \mathcal{D})$, we have

Theorem 2.1.

$$\begin{aligned} & \|\hat{w} - \hat{w}^{\max_k}\|_2^2 \\ \leq & \frac{2\hat{w}^T (\mathbf{I}_d - \mathbf{I}_d(k))}{\max\{\lambda_2 N_{E=1}, \lambda_3 N_{E=1}\}} \sum_{i:E_i=1} \left(\frac{\sum_{T_j \geq T_i} (x_i - x_j) \exp(x_j^T \hat{w}^{\max_k})}{\sum_{T_j \geq T_i} \exp(x_j^T \hat{w}^{\max_k})} \right), \end{aligned} \quad (4)$$

where \mathbf{I}_d is a $d \times d$ identity matrix, and $\mathbf{I}_d(k)$ denotes a $d \times d$ identity matrix with k ones on its diagonal.

Proof. Let $\hat{w}^{\max_k} = \mathbf{I}_d(k)\hat{w}$, and the gradient of the original loss function $\nabla\mathcal{L}$ computed at \hat{w}^{\max_k} is as follows:

$$\begin{aligned} & \nabla\mathcal{L}(\hat{w}^{\max_k}) \\ = & -\frac{1}{N_{E=1}} \sum_{i:E_i=1} \left(x_i - \frac{\sum_{T_j \geq T_i} x_j \exp(x_j^T \hat{w}^{\max_k})}{\sum_{T_j \geq T_i} \exp(x_j^T \hat{w}^{\max_k})} \right) \\ & - \frac{\lambda_2}{N_{E=1}} \sum_{i:E_i=1} \left(\mathbf{I}_d(k)x_i - \frac{\sum_{T_j \geq T_i} \mathbf{I}_d(k)x_j \exp(x_j^T \hat{w}^{\max_k})}{\sum_{T_j \geq T_i} \exp(x_j^T \hat{w}^{\max_k})} \right) + \lambda_3 \hat{w}^{\max_k}. \end{aligned} \quad (5)$$

Note that \hat{w} is the optimal solution to (3), so we have

$$\nabla\mathcal{L}(\hat{w}) = 0. \quad (6)$$

Then, we get

$$\begin{aligned} & \nabla\mathcal{L}(\hat{w}^{\max_k}) \\ = & \nabla\mathcal{L}(\hat{w}^{\max_k}) - \mathbf{I}_d(k)\nabla\mathcal{L}(\hat{w}) \\ = & -\frac{1}{N_{E=1}} \sum_{i:E_i=1} \left(x_i - \frac{\sum_{T_j \geq T_i} x_j \exp(x_j^T \hat{w}^{\max_k})}{\sum_{T_j \geq T_i} \exp(x_j^T \hat{w}^{\max_k})} \right) \end{aligned}$$

$$\begin{aligned}
& -\frac{\lambda_2}{N_{E=1}} \sum_{i:E_i=1} \left(\mathbf{I}_d(k)x_i - \frac{\sum_{T_j \geq T_i} \mathbf{I}_d(k)x_j \exp(x_j^T \hat{w}^{\max_k})}{\sum_{T_j \geq T_i} \exp(x_j^T \hat{w}^{\max_k})} \right) \\
& + \lambda_3 \hat{w}^{\max_k} - \lambda_3 \mathbf{I}_d(k)\hat{w} + \frac{\mathbf{I}_d(k)}{N_{E=1}} \sum_{i:E_i=1} \left(x_i - \frac{\sum_{T_j \geq T_i} x_j \exp(x_j^T \hat{w})}{\sum_{T_j \geq T_i} \exp(x_j^T \hat{w})} \right) \\
& + \frac{\lambda_2 \mathbf{I}_d(k)}{N_{E=1}} \sum_{i:E_i=1} \left(\mathbf{I}_d(k)x_i - \frac{\sum_{T_j \geq T_i} \mathbf{I}_d(k)x_j \exp(x_j^T \mathbf{I}_d(k)\hat{w})}{\sum_{T_j \geq T_i} \exp(x_j^T \mathbf{I}_d(k)\hat{w})} \right) \tag{7} \\
= & -\frac{1}{N_{E=1}} \sum_{i:E_i=1} \left(x_i - \frac{\sum_{T_j \geq T_i} x_j \exp(x_j^T \hat{w}^{\max_k})}{\sum_{T_j \geq T_i} \exp(x_j^T \hat{w}^{\max_k})} \right) \\
& + \frac{1}{N_{E=1}} \sum_{i:E_i=1} \left(\mathbf{I}_d(k)x_i - \frac{\sum_{T_j \geq T_i} \mathbf{I}_d(k)x_j \exp(x_j^T \hat{w})}{\sum_{T_j \geq T_i} \exp(x_j^T \hat{w})} \right).
\end{aligned}$$

Let

$$\theta = \frac{\hat{w}^{\max_k} - \hat{w}}{\|\hat{w}^{\max_k} - \hat{w}\|_2}. \tag{8}$$

Notice that \mathcal{L} is μ -strongly convex, thus, $\exists \mu > 0, \forall t > 0$, we obtain

$$\mathcal{L}(\hat{w}^{\max_k} - t\theta) - \mathcal{L}(\hat{w}^{\max_k}) \geq -t\theta^T \nabla \mathcal{L}(\hat{w}^{\max_k}) + \frac{\mu t^2}{2}. \tag{9}$$

Noting that \hat{w} is the optimal solution of $\mathcal{L}(\hat{w})$, we have

$$-\theta^T \nabla \mathcal{L}(\hat{w}^{\max_k}) + \frac{\mu t}{2} \leq 0. \tag{10}$$

Then we get

$$\|\hat{w}^{\max_k} - \hat{w}\|_2 \leq t \leq \frac{2}{\mu} \theta^T \nabla \mathcal{L}(\hat{w}^{\max_k}). \tag{11}$$

Plugging (7) and (8) into (11), we have

$$\begin{aligned}
& \|\hat{w}^{\max_k} - \hat{w}\|_2^2 \\
\leq & -\frac{2(\hat{w}^{\max_k} - \hat{w})^\top}{\mu N_{E=1}} \sum_{i:E_i=1} \left(x_i - \frac{\sum_{T_j \geq T_i} x_j \exp(x_j^\top \hat{w}^{\max_k})}{\sum_{T_j \geq T_i} \exp(x_j^\top \hat{w}^{\max_k})} \right) \\
& + \frac{2(\hat{w}^{\max_k} - \hat{w})^\top}{\mu N_{E=1}} \sum_{i:E_i=1} \left(\mathbf{I}_d(k) x_i - \frac{\sum_{T_j \geq T_i} \mathbf{I}_d(k) x_j \exp(x_j^\top \hat{w})}{\sum_{T_j \geq T_i} \exp(x_j^\top \hat{w})} \right) \\
= & \frac{2\hat{w}^\top (\mathbf{I}_d - \mathbf{I}_d(k))}{\mu N_{E=1}} \sum_{i:E_i=1} \left(x_i - \frac{\sum_{T_j \geq T_i} x_j \exp(x_j^\top \hat{w}^{\max_k})}{\sum_{T_j \geq T_i} \exp(x_j^\top \hat{w}^{\max_k})} \right). \tag{12}
\end{aligned}$$

160 Taking $\mu = \max\{\lambda_2, \lambda_3\}$, the proof follows. \square

Lemma 2.1. $\mathcal{L}(\hat{w})$ has a Lipschitz continuous gradient with Lipschitz constant L .

Proof. We compute the Hessian matrix of $\mathcal{L}(\hat{w})$ in (3) as follows:

$$\begin{aligned}
& \nabla^2 \mathcal{L}(\hat{w}) \\
= & -\partial \left[\frac{1}{N_{E=1}} \sum_{i:E_i=1} \left(x_i - \frac{\sum_{T_j \geq T_i} x_j \exp(x_j^\top \hat{w})}{\sum_{T_j \geq T_i} \exp(x_j^\top \hat{w})} \right) \right] / \partial \hat{w} \\
& -\partial \left[\frac{\lambda_2}{N_{E=1}} \sum_{i:E_i=1} \left(\mathbf{I}_d(k) x_i - \frac{\sum_{T_j \geq T_i} \mathbf{I}_d(k) x_j \exp(x_j^\top \mathbf{I}_d(k) \hat{w})}{\sum_{T_j \geq T_i} \exp(x_j^\top \mathbf{I}_d(k) \hat{w})} \right) \right] / \partial \hat{w} \\
& + \lambda_3. \tag{13}
\end{aligned}$$

Then, by Minkowski's inequality [27], we easily get

$$\begin{aligned}
& \|\nabla^2 \mathcal{L}(\hat{w})\|_2 \\
\leq & \left\| \frac{1}{N_{E=1}} \sum_{i:E_i=1} \left(\frac{\sum_{T_j \geq T_i} x_j^T x_j \exp(x_j^T \hat{w})}{\sum_{T_j \geq T_i} \exp(x_j^T \hat{w})} \right) \right. \\
& - \frac{1}{N_{E=1}} \sum_{i:E_i=1} \left(\frac{\left(\sum_{T_j \geq T_i} x_j^T \exp(x_j^T \hat{w}) \right) \left(\sum_{T_j \geq T_i} x_j \exp(x_j^T \hat{w}) \right)}{\left(\sum_{T_j \geq T_i} \exp(x_j^T \hat{w}) \right)^2} \right) \left. \right\|_2 \\
& + \left\| \frac{\lambda_2}{N_{E=1}} \sum_{i:E_i=1} \left(\frac{\sum_{T_j \geq T_i} x_j^T x_j \exp(x_j^T \hat{w}^{\max_k})}{\sum_{T_j \geq T_i} \exp(x_j^T \hat{w}^{\max_k})} \right) - \frac{\lambda_2}{N_{E=1}} \sum_{i:E_i=1} \right. \\
& \left. \left(\frac{\left(\sum_{T_j \geq T_i} x_j^T \mathbf{I}_d(k) \exp(x_j^T \hat{w}^{\max_k}) \right) \left(\sum_{T_j \geq T_i} \mathbf{I}_d(k) x_j \exp(x_j^T \hat{w}^{\max_k}) \right)}{\left(\sum_{T_j \geq T_i} \exp(x_j^T \hat{w}^{\max_k}) \right)^2} \right) \right\|_2 \\
& + \lambda_3 \\
\leq & (1 + \lambda_2) \max_{T_j \geq T_i} \|x_j^T\|_2 + \lambda_3
\end{aligned} \tag{14}$$

Take $L = (1 + \lambda_2) \max_{T_j \geq T_i} \{\|x_j^T\|_2\} + \lambda_3$, the proof follows. \square

Lemma 2.2 ([28]). *If a function $f(\cdot)$ is differentiable on $\mathbb{R}^{d \times 1}$ and has an L -Lipschitz gradient, then $\forall \mathbf{x}, \mathbf{y} \in \mathbb{R}^{d \times 1}$, we have*

$$|f(\mathbf{y}) - f(\mathbf{x}) - (\mathbf{y} - \mathbf{x})^T \nabla f(\mathbf{x})| \leq \frac{L}{2} \|\mathbf{y} - \mathbf{x}\|_2^2. \tag{15}$$

Lemma 2.3.

$$\frac{\theta^T \nabla \mathcal{L}(\hat{w}^{\max_k})}{L} \leq \|\hat{w} - \hat{w}^{\max_k}\|_2. \tag{16}$$

Proof. By Lemma 2.2, $\forall \delta \geq 0$, we have the following inequality

$$\mathcal{L}(\hat{w}^{\max_k} - \delta\theta) - \mathcal{L}(\hat{w}^{\max_k}) \leq -\delta\theta^T \nabla \mathcal{L}(\hat{w}^{\max_k}) + \frac{L\delta^2}{2}. \quad (17)$$

By $\|\theta\| = 1$ and Lemma 2.1, we have

$$\begin{aligned} & \frac{\partial(-\delta\theta^T \nabla \mathcal{L}(\hat{w}^{\max_k}) + \frac{L\delta^2}{2})}{\partial \delta} \\ &= -\theta^T \nabla \mathcal{L}(\hat{w}^{\max_k}) + L\delta \\ &\geq -\theta^T \mathcal{L}(\hat{w}^{\max_k} - \delta\theta) \\ &= \frac{\partial(\mathcal{L}(\hat{w}^{\max_k} - \delta\theta) - \mathcal{L}(\hat{w}^{\max_k}))}{\partial \delta} \end{aligned} \quad (18)$$

And note that \hat{w} is the optimal solution, so $-\theta^T \nabla \mathcal{L}(\hat{w}^{\max_k}) \leq 0$. Then we can easily get

$$\begin{aligned} & \arg \min_{\delta > 0} \left\{ -\delta\theta^T \nabla \mathcal{L}(\hat{w}^{\max_k}) + \frac{L\delta^2}{2} \right\} \\ &\leq \arg \min_{\delta > 0} \{ \mathcal{L}(\hat{w}^{\max_k} - \delta\theta) - \mathcal{L}(\hat{w}^{\max_k}) \}. \end{aligned} \quad (19)$$

Finally, we calculate the minima on the left and right sides of (19) as follows:

$$\arg \min_{\delta > 0} \left\{ -\delta\theta^T \nabla \mathcal{L}(\hat{w}^{\max_k}) + \frac{L\delta^2}{2} \right\} = \frac{\theta^T \nabla \mathcal{L}(\hat{w}^{\max_k})}{L}, \quad (20)$$

and

$$\arg \min_{\delta > 0} \{ \mathcal{L}(\hat{w}^{\max_k} - \delta\theta) - \mathcal{L}(\hat{w}^{\max_k}) \} = \|\hat{w}^{\max_k} - \hat{w}\|_2, \quad (21)$$

then we complete the proof. \square

Theorem 2.2.

$$\begin{aligned} & \|\hat{w} - \hat{w}^{\max_k}\|_2^2 \\ &\geq \frac{\hat{w}^T (\mathbf{I}_d - \mathbf{I}_d(k))}{((1 + \lambda_2)C_1 + \lambda_3)N_{E=1}} \sum_{i: E_i=1} \left(\frac{\sum_{T_j \geq T_i} (x_i - x_j) \exp(x_j^T \hat{w}^{\max_k})}{\sum_{T_j \geq T_i} \exp(x_j^T \hat{w}^{\max_k})} \right). \end{aligned} \quad (22)$$

Proof. By (7) and (8), we have

$$\begin{aligned}
& \frac{\theta^T \nabla \mathcal{L}(\hat{w}^{\max_k})}{L \|\hat{w}^{\max_k} - \hat{w}\|_2} \\
&= \frac{(\hat{w}^{\max_k} - \hat{w})^T \nabla \mathcal{L}(\hat{w}^{\max_k})}{L \|\hat{w}^{\max_k} - \hat{w}\|_2} \\
&= -\frac{(\hat{w}^{\max_k} - \hat{w})^T}{L \|\hat{w}^{\max_k} - \hat{w}\|_2 N_{E=1}} \sum_{i:E_i=1} \left(x_i - \frac{\sum_{T_j \geq T_i} x_j \exp(x_j^T \hat{w}^{\max_k})}{\sum_{T_j \geq T_i} \exp(x_j^T \hat{w}^{\max_k})} \right) \\
&\quad + \frac{(\hat{w}^{\max_k} - \hat{w})^T}{L \|\hat{w}^{\max_k} - \hat{w}\|_2 N_{E=1}} \sum_{i:E_i=1} \left(\mathbf{I}_d(k) x_i - \frac{\sum_{T_j \geq T_i} \mathbf{I}_d(k) x_j \exp(x_j^T \hat{w})}{\sum_{T_j \geq T_i} \exp(x_j^T \hat{w})} \right) \\
&= \frac{\hat{w}^T (\mathbf{I}_d - \mathbf{I}_d(k))}{L \|\hat{w}^{\max_k} - \hat{w}\|_2 N_{E=1}} \sum_{i:E_i=1} \left(x_i - \frac{\sum_{T_j \geq T_i} x_j \exp(x_j^T \hat{w}^{\max_k})}{\sum_{T_j \geq T_i} \exp(x_j^T \hat{w}^{\max_k})} \right). \tag{23}
\end{aligned}$$

By Lemmas 2.1 and 2.3, we get

$$\begin{aligned}
& \|\hat{w} - \hat{w}^{\max_k}\|_2^2 \\
&\geq \frac{\hat{w}^T (\mathbf{I}_d - \mathbf{I}_d(k))}{LN_{E=1}} \sum_{i:E_i=1} \left(x_i - \frac{\sum_{T_j \geq T_i} x_j \exp(x_j^T \hat{w}^{\max_k})}{\sum_{T_j \geq T_i} \exp(x_j^T \hat{w}^{\max_k})} \right) \\
&\geq \frac{\hat{w}^T (\mathbf{I}_d - \mathbf{I}_d(k))}{((1 + \lambda_2)C_1 + \lambda_3)N_{E=1}} \sum_{i:E_i=1} \left(x_i - \frac{\sum_{T_j \geq T_i} x_j \exp(x_j^T \hat{w}^{\max_k})}{\sum_{T_j \geq T_i} \exp(x_j^T \hat{w}^{\max_k})} \right), \tag{24}
\end{aligned}$$

165 then we complete the proof. \square

From Theorems 2.1 and 2.2, it is observed that the proved error bound of $\|\hat{w} - \hat{w}^{\max_k}\|_2^2$ tight up to constant factors. Further, it implies that there is a close relationship between $\|\hat{w} - \hat{w}^{\max_k}\|_2^2$ and $\|\mathbf{I}_d(k) - \mathbf{I}_d\|_2$. Based on this intuition, we have the following corollary:

Corollary 2.1. *Let $\sup_{w \in \mathbb{R}^{d \times 1}} \|w\|_2 \leq C_0$, then we have*

$$\|\hat{w} - \hat{w}^{\max_k}\|_2^2 \leq \frac{4C_0C_1\sqrt{d-k}}{\max\{\lambda_2, \lambda_3\}}. \quad (25)$$

170 *Proof.* By applying the non-negative property of exponential function and the sub-multiplicativity, the proof follows. \square

From Corollary 2.1, it is clear that the error of $\|\hat{w} - \hat{w}^{\max_k}\|_2^2$ can be reduced by increasing the regularization parameters λ_2 and λ_3 appropriately; meanwhile, it can also make the error smaller by increasing k , which can be observed from
 175 Supplementary Figures C.6, D.8, and E.10, and they show a general upward trend with the increasement of k . Despite the useful insights obtained from the bound in (25), it is noted that the upper bound in (25) might not be very tight because of the uniform upper bound for $w \in \mathbb{R}^{d \times 1}$. When there is additional information on w , such as sparsity or group-level sparsity, we may further im-
 180 prove the upper found in (25). We leave this as a line of future study while presenting a possible improvement below.

Potential for improvement. Next, we mathematically analyze that our algorithm has room for further improvement in some cases.

If we use the selected variables to re-train the Max_k part in the EXCEL-extended models, the performance might be improved. Such a fact is revealed by the following Theorem. For simplicity, let

$$A(f) = -\frac{\lambda_0}{N_{E=1}} \sum_{i: E_i=1} \left(f(W_I x_i) - \log \sum_{T_j \geq T_i} \exp f(W_I x_i) \right),$$

and

$$B(f) = -\frac{\lambda_2}{N_{E=1}} \sum_{i: E_i=1} \left(f(W_I^{\max_k} x_i) - \log \sum_{T_j \geq T_i} \exp f(W_I^{\max_k} x_i) \right).$$

Theorem 2.3. *Let (f^*, W_I^*) be an optimal solution of (3). If $\text{Pos}(W_I^* - (W_I^*)^{\max_k}) >$*

0, then there exists $f^{*'}$, such that

$$B(f^{*'}) \leq B(f^*),$$

185 where $\text{Pos}(W)$ counts the number of positive values in W .

Proof. Assume that, for any $f^{*''}$,

$$B(f^{*''}) > B(f^*).$$

If f^* is the optimal solution of A , noting that $\text{Pos}(W_1^* - (W_1^*)^{\max_k}) > 0$, then there exists $f^{*'''}$, such that

$$B(f^{*'''}) \leq B(f^*).$$

This contradicts our assumption. □

3. Experimental results

Next, we apply EXCEL to two semi-synthetic datasets and three real-world survival datasets, including clinical and genetic data, with varying numbers of
190 subjects and variables and portions of censored observations. We will demonstrate that our proposed EXCEL approach can identify critically important risk factors from thousands of variables potentially related to the survival time and, with only a small subset of identified variables, it can achieve prognostic performance comparable to or better than the original models with all variables.

195 *Semi-synthetic data.* We first benchmark our EXCEL approach by embedding it as a pluggable module into the standard CPH model with two semi-synthetic datasets. These datasets allow for straightforward visual inspection of selected features. Also, we compare the applications of our approach with two baselines, the standard CPH model and the more recent algorithm, BeSS. We will use

200 R function `bess.one()`, which aims to solve the best subset selection problem with a specified cardinality.

1) We use the pixels of handwritten digits 3 and 8 in USPS [29] as variables and generate synthetic survival times for them using the exponential distribution, following the way of [30, 31, 32] for constructing survMNIST.⁴ The resultant data is called `SurvUSPS_3vs8`.
205

2) For digits 3 and 8 in USPS, firstly, we resize the original 16×16 images into 28×28 images by extending each boundary by 6 pixels and filling in uniform noise. Then, we follow the way in 1) to assign survival times for them. The resultant data is called `NSurvUSPS_3vs8`.

210 On `NSurvUSPS_3vs8`, we compare the standard CPH model, BeSS for the best subset selection in CPH model, and Max_k -CPH. Randomly sampled images are illustrated in Figure 3 (a). It is found that many variables selected by the baseline CPH model are located in the noise boundary regions (see Figure 3 (b) and (c)), while those selected by BeSS and Max_k -CPH are salient points distinguishing the digits 3 and 8 (see Figure 3 (d)-(g)). These results
215 indicate that BeSS and our proposed method can identify important variables and eliminate noise.

On `SurvUSPS_3vs8`, we randomly split all samples 10 times by a ratio of 80:20 for training and test sets, and then we use the three models to perform
220 variable selection. The experimental results are demonstrated in Figure 3 (i)-(k). It is clear that the variables selected by Max_k -CPH essentially overlap for different splits, whereas those by the baselines do not overlap well. These results reveal that the features selected by our EXCEL method are more stable compared to those by the baselines.

225 Next, we will implement a variety of experiments on real-world datasets, and relevant statistics of these datasets are shown in Supplementary Table A.2.

⁴We randomly assigned each class label to a risk group, so that one digit would correspond to better survival and the other to worse survival. Then, we generate a risk score that indicates how risky it is to experience an event, relative to others. For more details, see the links of Semi-synthetic data in Section **Data availability**.

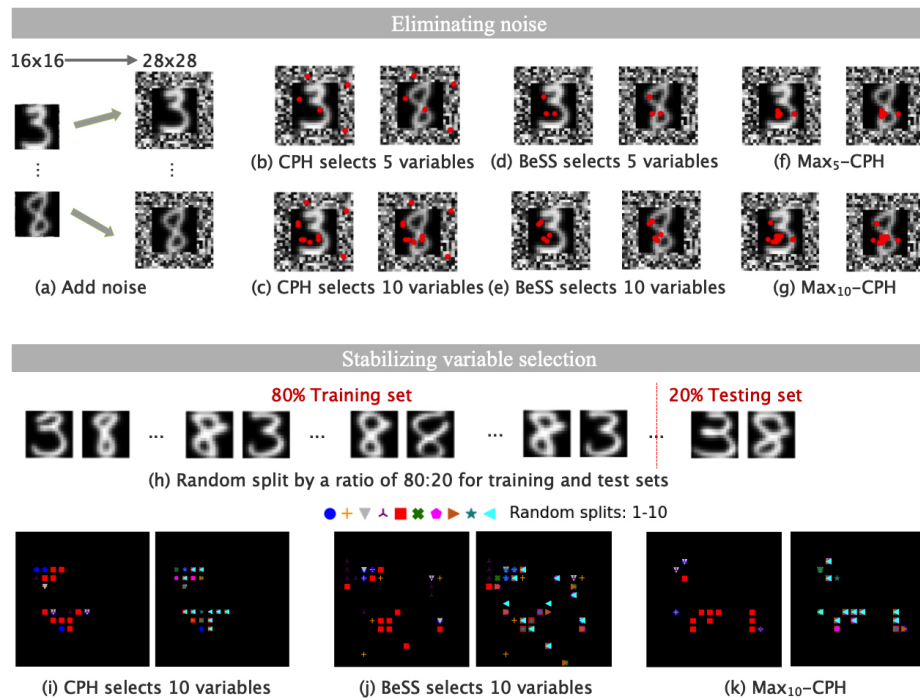


Figure 3: Experiments on two semi-synthetic datasets. (a)-(g) Noise elimination analysis of different methods with $k = 5$ and 10 on NSurvUSPS_3vs8; (h) Illustration of random splitting for training and test sets; (i)-(k) Stability analysis of variable selection by different methods with 5 (left in each pair of images) and 10 (right in each pair of images) random splits for $k = 10$.

Breast cancer dataset. We directly import the function `sksurv.datasets.load_breast_cancer()`⁵ to download this dataset [33]. It contains the expression levels of 76 genes, age, estrogen receptor status (denoted by `er`), tumor size, and grade for 198 subjects. First, we perform one-hot encoding for categorical variables of `er` and grade; then, we apply CPH, DeepSurv, Cox-nnet, and their EXCEL-embedded counterparts to analyze this dataset. The results for k from 5 to 40 with a step size of 5 are shown in Supplementary Figure C.6(a)-(c). Using the number of selected variables corresponding to the optimal CI, we apply the EXCEL-extended models by setting k to the best numbers of selected variables to calculate IBS in Supplementary Figure C.6(e)-(g). It is observed that the EXCEL-extended survival models, with fractions of selected variables, can achieve comparable or better performance than their counterparts without EXCEL. Moreover, the EXCEL-extended models can identify a subset of critical variables for achieving maximal performance. We provide the top 10 variables selected by the best model, i.e., Max₃₅-DeepSurv, in Table 1.

Table 1: Top 10 variables selected by EXCEL-extended survival models on three datasets.

Dataset Rank	Breast cancer	SUPPORT	GBM
1	<i>X204540_at</i>	slos	AGE
2	<i>X202240_at</i>	sfdm2_<2 mo. follow-up	<i>HIST3H2A</i>
3	<i>X203306_s_at</i>	sex_female	<i>PRODH</i>
4	<i>X218883_s_at</i>	sex_male	<i>CCBL2</i>
5	er	ca_metastatic	<i>ATP10B</i>
6	<i>X202239_at</i>	sfdm2_no (M2 and SIP pres)	<i>FZD7</i>
7	<i>X202687_s_at</i>	sfdm2_adl>=4 (>=5 if sur)	<i>TPM4</i>
8	<i>X204014_at</i>	avtisst	<i>NMB</i>
9	<i>X208180_s_at</i>	dzgroup_Lung Cancer	<i>RPS4Y1</i>
10	<i>X207118_s_at</i>	sfdm2_SIP>=30	<i>PACSI</i>

For quantifying the significance of selected variables, we use k -means clustering to cluster the subjects into two groups according to the selected variables, and then we use the KM estimator to estimate the survival functions and the

⁵See the link: https://scikit-survival.readthedocs.io/en/latest/api/generated/sksurv.datasets.load_breast_cancer.html

245 Log-rank test to calculate p-values for the groups according to each of the individual variables. The top 10 variables identified by this clustering-then-test approach are as follows (the values in the parentheses are p-values): *X202240_at* (6.1E-05), *X202418_at* (2.3E-03), *X202687_s_at* (9.5E-03), *X203306_s_at* (5.8E-03), *X204014_at* (4.5E-03), *X204015_s_at* (9.8E-03), *X208180_s_at* (1.8E-03),
250 *X211762_s_at* (3.8E-03), *er* (9.6E-03), and *X205034_at* (1.5E-02). In [34], two methods were proposed, C-based splitting and log-rank splitting, to select variables on this dataset. Four variables (*X202240_at*, *X204014_at*, *X204015_s_at*, and *er*) selected by its former method and two variables (*X202240_at* and *X204014_at*) by the latter are of statistical significance. In Table 1, it is seen that six
255 (*X202240_at*, *X202687_s_at*, *X203306_s_at*, *X204014_at*, *X208180_s_at*, and *er*) of the top 10 variables identified by Max_{35} -DeepSurv have statistical significance. We depict the KM survival curves for the top 3 variables identified by Max_{35} -DeepSurv in Supplementary Figure C.7 (a)-(c) and the scatter plots with 95% confidence intervals for pairwise groups for different individual variables in
260 Supplementary Figure C.7 (d)-(f). These figures indicate that the two groups obtained from each of the top 3 variables are well separated in survival times, suggesting these variables' high predictive ability. Here, it is noted that the KM curve of Group 1 for the top feature in Supplementary Figure C.7 (a) plummets sharply after about time 7,000 (indicating the deaths of all subjects in this
265 group) while Group 2 does not, which illustrates the close association of this feature with the patent difference between the 2 groups' survival times. It is worth pointing out that, nonetheless, KM curves in Supplementary Figure C.7 (a) have a larger p-value than the two lower-ranked features in Supplementary Figure C.7 (b)-(c), which appears to be a limitation of the Log-rank test (that
270 is, it can only indicate whether the 2 groups are of the same distribution but not the size of the difference [35]) yet a strength of EXCEL.

Study to Understand Prognoses and Preferences for Outcomes and Risks of Treatments (SUPPORT) dataset. To analyze models on real clinical data, we use a common benchmark dataset in the survival analysis SUPPORT [36]. This

275 dataset contains demographic, score data acquired from patients diagnosed with
cancer, chronic obstructive pulmonary disease, cirrhosis, acute renal failure,
multiple organ system failure, sepsis, and so on. We preprocess this dataset fol-
lowing [32] and obtain the resultant dataset with 9,105 subjects and 59 variables.
Then we compare different models and show the corresponding results for k from
280 5 to 40 with a step size of 5 in Supplementary Figure D.8 (a)-(c), and the IBS
by the EXCEL-embedded models with the best numbers of selected variables in
Supplementary Figure D.8 (d)-(g). It is observed that EXCEL-extended models
achieve comparable or better performance when a certain number of variables
are selected, and the subset of top 10 critical variables for the best model,
285 Max₂₅-Cox-nnet, is given in Table 1.

Also, we adopt k -means clustering to cluster the subjects into two groups
according to each of the top 3 selected variables; then, on each resultant group,
we perform the KM estimation and Log-rank test. The results are shown in Sup-
plementary Figure D.9. Each of these variables clearly exhibits high predictive
290 ability for survival time.

Glioblastoma multiforme (GBM) cancer dataset. Obtained from the Cancer
Genome Atlas (TCGA, <http://cancergenome.nih.gov>), this dataset contains gene
expression and clinical data. We preprocess the data following [4] to obtain 5,567
genes, 860 pathways, and clinical data of ages from 522 subjects for our analysis.
295 The pathway data are mainly used for Cox-PASnet [4] and its EXCEL-extended
counterpart. For other models, we only use the combined data of gene variables
and one clinical variable, AGE, as input without any pathway information. We
compare different models with k ranging from 100 to 1000 with a step size
of 100, showing the results in Supplementary Figure E.10 (a)-(c) and (g) and
300 the corresponding IBS by the embedded models with the best numbers of se-
lected variables in Supplementary Figure E.10 (d)-(f) and (h). It is observed
that Max₈₀₀-DeepSurv achieves the best performance when 800 variables are
selected, from which the top 10 critical variables are given in Table 1.

Further, we adopt k -means clustering to cluster the subjects into two groups

305 according to each of the top 3 selected variables; then, we perform the KM
estimation and Log-rank test for each obtained group. The results shown in
Supplementary Figure E.11 indicate that each of these selected variables is well
separable for the subjects and of high predictive ability for the survival time.
More detailed results about CI and IBS for these datasets are provided in Sup-
310 plementary Tables B.3 and B.4.

4. Discussion

Real-world survival data, such as gene expression, is often high-dimensional
with a much larger number of covariates than the subjects. For computational
feasibility and explainability of learning, we propose a plug-and-play approach
315 that can be easily used with the existing DL-based survival models for variable
selection.

Reducing the number of variables for learning. Structurally, our EXCEL ap-
proach uses the operator Max_k to pinpoint k most predictive variables, which
introduces a sub-architecture into the architecture of existing models. The in-
320 duced sub-architecture has a fitting error term similar to the existing models,
and it is trained cooperatively with the architecture of existing models. By re-
garding the existing model as a regularization term, we observe that the result-
ing sub-model can select critical variables while capturing the complex nonlinear
relationship between input variables and survival time. As empirically shown
325 above and summarized in Figure 4, this concise approach for regularization is
able to select the most predictive k variables to enhance the learning ability of
the survival model, achieving prediction performance on par with or better than
strong baseline methods. By discarding noise or less informative variables and
identifying useful variables of long-term prognostic values, our easily deployable
330 approach can help facilitate explainability to the DL-based models and facilitate
their prediction, especially on high-dimensional data.

Explainability of model learning. Our EXCEL approach brings explainability to
model learning. Taking the Breast cancer dataset as an example, the clinical

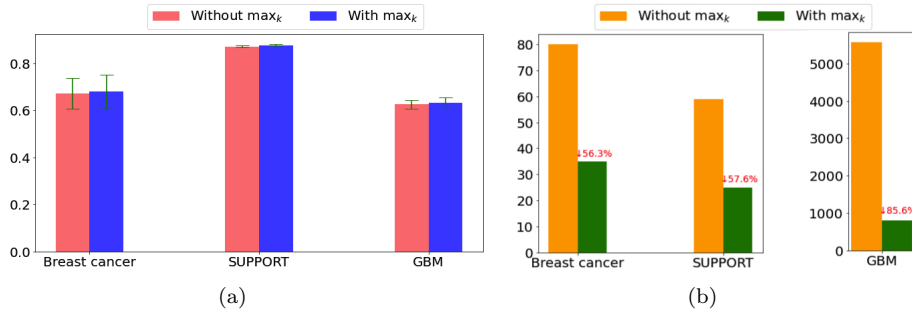


Figure 4: Performance and the number of used variables on Breast cancer (DeepSurv and Max_k -DeepSurv), SUPPORT (Cox-nnet and Max_k -Cox-nnet), and GBM (DeepSurv and Max_k -DeepSurv). (a) The comparison of performance (in CI) with and without Max_k ; (b) The numbers of variables used in our models compared to the full numbers in the original models.

variable “er” is identified as one of the top 5 important variables; in the literature, the status of estrogen receptor has been confirmed to associate with the risk of breast cancer [37, 38]. Also, take the GBM dataset as another example. GBM cancer is one of the most aggressive, malignant brain tumors with a poor prognosis [39]. During learning, we use the clinical variable “AGE” together with more than 5,000 gene expressions as input. Our Max_{800} -DeepSurv identifies 800 important variables out of 5,568 variables, with the most important 3 variables being AGE, *HIST3H2A*, and *PRODH*. In the literature, age was identified as a significant covariate for the prognosis of GBM [40, 41]; *HIST3H2A* was reported as a differentially expressed gene in many studies, e.g., [42, 40, 43]; *PRODH* was also found to be linked with GBM cancer in [44].

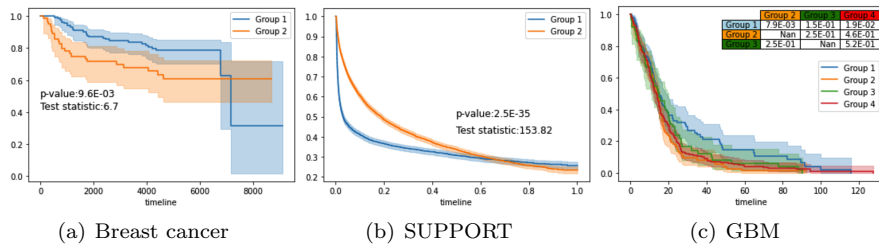


Figure 5: Survival curves by KM estimator with Log-rank tests for all selected variables by Max_{35} -DeepSurv, Max_{25} -Cox-nnet, and Max_{800} -DeepSurv. The shaded areas in (a)-(c) show the 95% confidence interval.

345 *Predictability of the selected subset of variables.* For further analyzing the significance of selected variables, we use k -means clustering to cluster the subjects into two groups according to the subsets of variables selected by Max₃₅-DeepSurv, Max₂₅-Cox-nnet, and Max₈₀₀-DeepSurv, respectively; then we apply the KM estimator and Log-rank test to the groups, with the results shown in Figure 5. 350 The p-values for Breast cancer and SUPPORT datasets are 9.6E-03 and 2.5E-35, indicating significant differences between the KM curves based on EXCEL-selected variables. For the dataset GBM, the number of the original variables is large, out of which 800 variables are selected as the most predictive for survival times. Subsequently, we use k -means clustering to cluster the subjects into four 355 groups according to these variables. The p-values of two pairwise groups are significant, i.e., 7.9E-03 for group 1 vs. group 2 and 1.9E-02 for group 1 vs. group 4, each of which indicates a significant difference between the KM curves for these groups.

5. Conclusion

360 While crucial to explainability, it is challenging to reveal the associations between highly nonlinear, high-dimensional, and low-sample size data, such as genetic and clinical dataset, and the survival time in survival analysis. Nonlinear survival methods, including DL-based models, can well model high-level interactions; nonetheless, they typically work as a black-box, lacking interpretation 365 and needed explainability. Thus, transparent learning and accurate prediction of survival time based on patients' critical variables are urgent, unmet needs. A solution can help identify new intervention targets and potentially improve patient care and treatment practice. In this paper, we are interested in understanding how the survival models yield predictions on right censored data. To 370 this end, we propose a novel approach, EXCEL, to identify critical variables of long term prognostic values and simultaneously implement deep model training based on these identified variables. In a wide variety of experiments, including two semi-synthetic datasets, one toy dataset, and three clinical and/or genetic

datasets, we demonstrate the effectiveness of our proposed explainable censored
375 learning or finding critical features and making survival predictions.

This paper focuses on a practical algorithm that can plug and play on exist-
ing DL-based survival models, and we will further study its theoretical properties
in our future work.

Funding

380 This work was partially supported by the NIH grants R21AG070909, R56NS117587,
R01HD101508, P30 AG072496, and ARO W911NF-17-1-0040.

Appendix A. Datasets

Table A.2: Statistics of used datasets.

Statistics Dataset	#Sample	#Variable	%Censored
Breast cancer	198	80	74.24
SUPPORT	9,105	59	31.89
GBM	522	5,568	14.37

Appendix B. Appendix

Appendix B.1. CI of Different Methods

Table B.3: CI of compared methods.

Dataset Method	Breast cancer	SUPPORT	GBM
CPH	0.653±0.072	0.842±0.004	0.614±0.021
Max _k -CPH	<i>k</i> :40, 0.638±0.077	<i>k</i> :35, 0.842±0.004	<i>k</i> :300, 0.623±0.015
DeepSurv	0.672±0.065	0.828±0.003	0.625±0.018
Max _k -DeepSurv	<i>k</i> :35, 0.679± 0.072	<i>k</i> :30, 0.830± 0.003	<i>k</i> :800, 0.633± 0.021
Cox-nnet	0.672± 0.066	0.871±0.005	0.526± 0.043
Max _k -Cox-nnet	<i>k</i> :15, 0.678±0.057	<i>k</i> :25, 0.876± 0.005	<i>k</i> :800, 0.534±0.049
PASNet	\	\	0.574±0.054
Max _k -PASNet	\	\	<i>k</i> :100, 0.580±0.019

Table B.4: IBS of compared methods.

Dataset Method	Breast cancer	SUPPORT	GBM
CPH	0.174±0.021	0.260± 0.006	0.392±0.028
Max _k -CPH	0.176±0.023	0.260± 0.006	0.359±0.023
DeepSurv	0.174±0.017	0.266±0.004	0.337±0.019
Max _k -DeepSurv	0.173±0.018	0.265±0.005	0.340± 0.020
Cox-nnet	0.174±0.018	0.269±0.007	0.346±0.019
Max _k -Cox-nnet	0.174±0.021	0.264±0.007	0.346±0.019
PASNet	\	\	0.351± 0.018
Max _k -PASNet	\	\	0.362±0.023

Appendix C. Different Methods on Breast Cancer

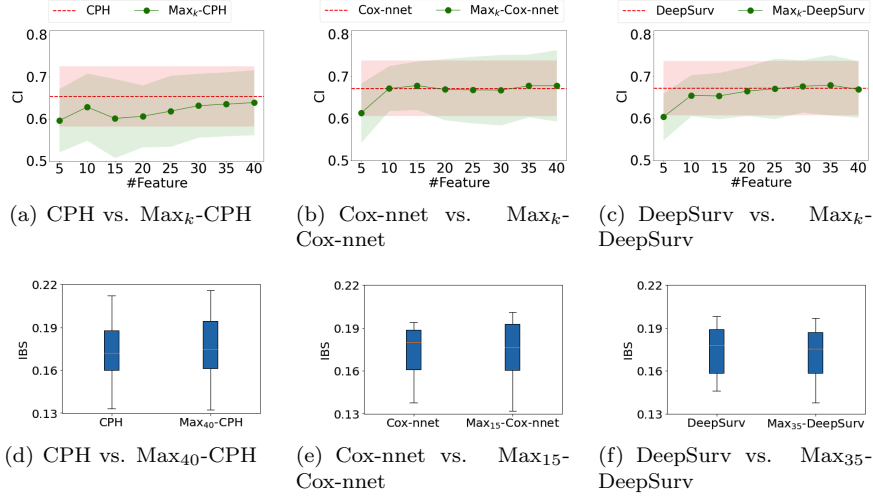


Figure C.6: Prediction performance, in CI (higher, better) and IBS (lower, better), of different methods on breast cancer dataset. The shaded areas in (a)-(c) show the fluctuations in standard error; the orange lines in (d)-(f) show the medians. For (a)-(c), the horizontal axis is only meaningful for the EXCEL-extended models.

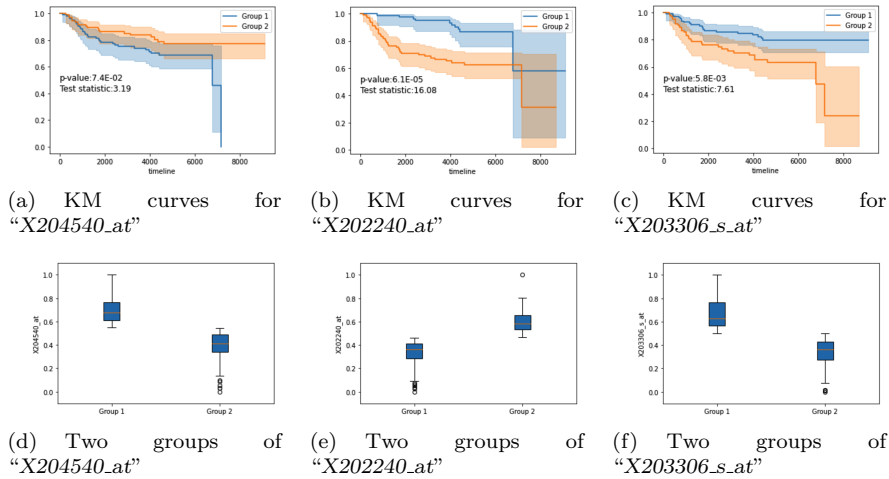


Figure C.7: KM survival curves and pairwise groups for the top 3 variables selected by Max_{35} -DeepSurv on the breast cancer dataset. The shaded areas in (a)-(c) show the 95% confidence intervals; the orange lines in (d)-(f) show the medians.

Appendix D. Different Methods on SUPPORT

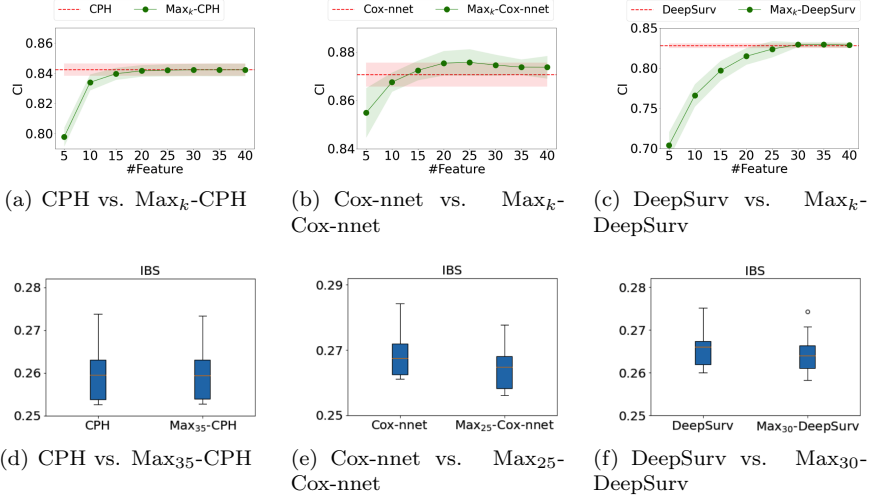


Figure D.8: Prediction performance, in CI (higher, better) and IBS (lower, better), of different methods on SUPPORT. The shaded areas in (a)-(c) show the fluctuations in standard error; the orange lines in (d)-(f) show the medians. For (a)-(c), the horizontal axis is only meaningful for the EXCEL-extended models.

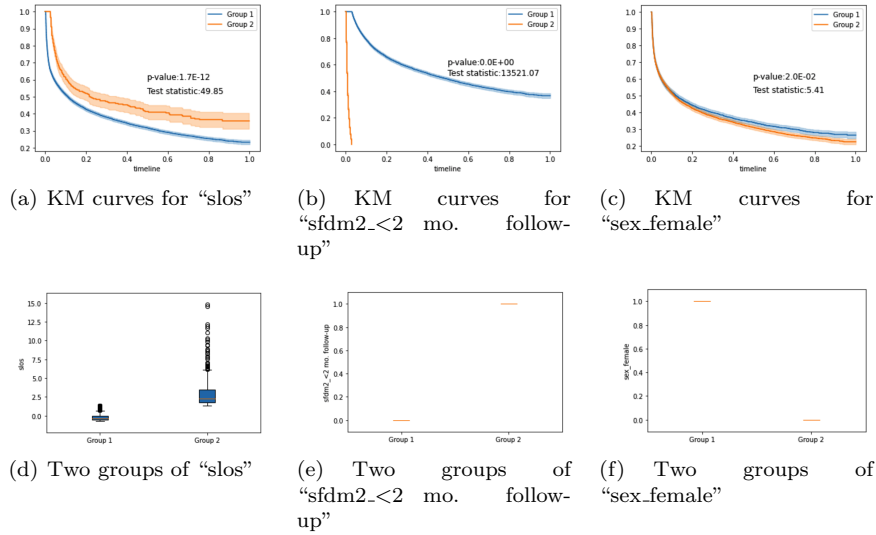


Figure D.9: KM survival curves and pairwise groups for the top 3 variables selected by Max₂₅-Cox-nnet on SUPPORT. The shaded areas in (a)-(c) show the 95% confidence intervals; the orange lines in (d)-(f) show the medians.

Appendix E. Different Methods on GBM

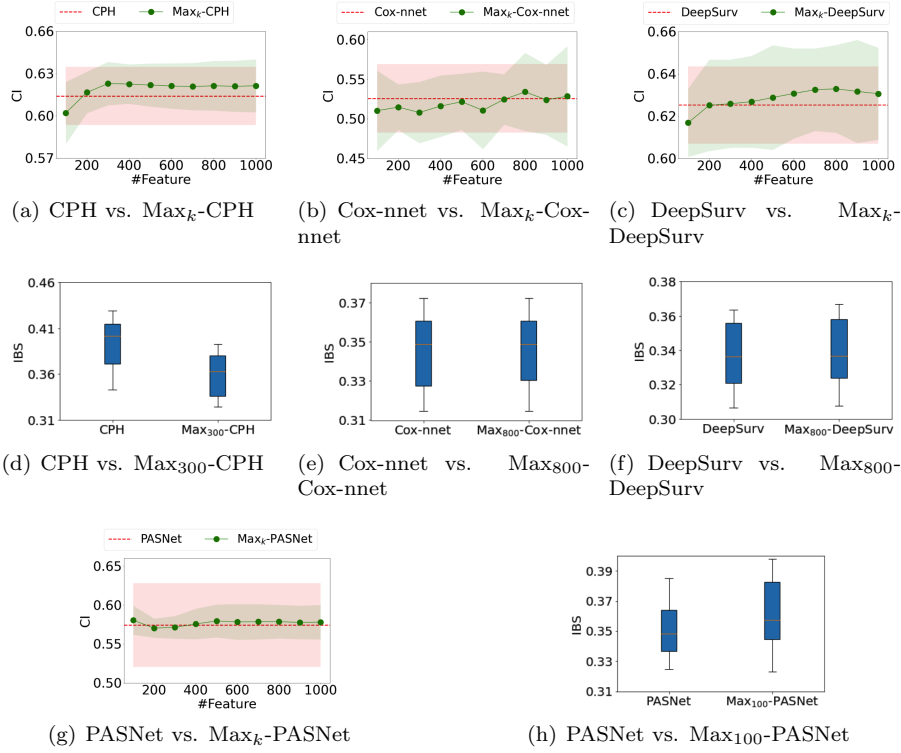


Figure E.10: Prediction performance, in CI (higher, better) and IBS (lower, better), of different methods on GBM. The shaded areas in (a)-(c) and (g) show the fluctuations in standard error; the orange lines in (d)-(f) and (h) show the medians. For (a)-(c) and (g), the horizontal axis is only meaningful for the EXCEL-extended models.

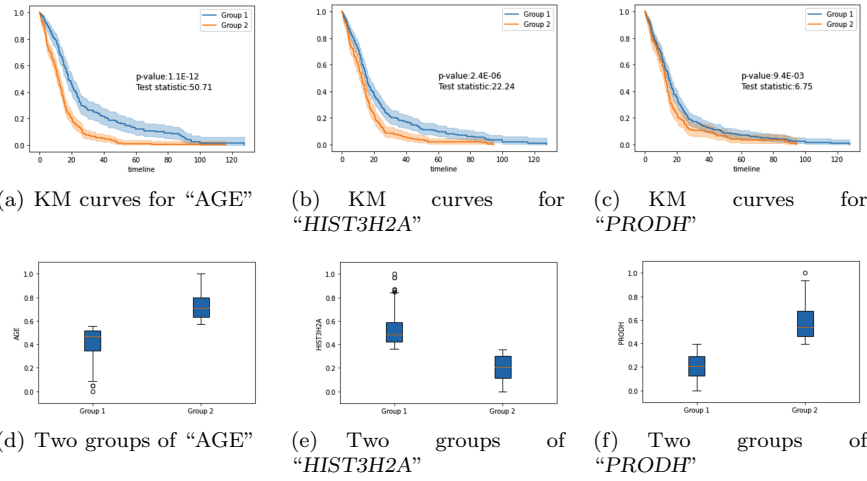


Figure E.11: KM survival curves and pairwise groups for the top 3 variables selected by Max₈₀₀-DeepSurv on GBM. The shaded areas in (a)-(c) show the 95% confidence intervals; the orange lines in (d)-(f) show the medians.

Appendix F. Details of Datasets WHAS500 and SUPPORT

Table F.5: WHAS500.

Variable	Description	Codes / Values
afb	Atrial Fibrillation	0 = No, 1 = Yes
age	Age at Hospital Admission	Years
av3	Complete Heart Block	0 = No, 1 = Yes
bmi	Body Mass Index	kg/m ²
chf	Congestive Heart Complications	0 = No, 1 = Yes
cvd	History of Cardiovascular Disease	0 = No, 1 = Yes
diasbp	Initial Diastolic Blood Pressure	mmHg
gender	Gender	0 = Male, 1 = Female
hr	Initial Heart Rate	Beats per minute
los	Length of Hospital Stay	Days from Hospital Admission to Hospital Discharge
miord	MI Order	0 = First, 1 = Recurrent
mitype	MI Type	0 = non Q-wave, 1 = Q-wave
sho	Cardiogenic Shock	0 = No, 1 = Yes
sysbp	Initial Systolic Blood Pressure	mmHg

Table F.6: SUPPORT.

Variable	Description	Codes / Values
slos	Days from Study Entry to Discharge	Days
sfdm2_<2 mo. follow-up	Patient died before 2 months after study entry	1= 2 mo. follow-up
sex_female	\	1 = Female
sex_male	\	1 = male
ca_metastatic	Cancer status	1= metastatic
sfdm2_no (M2 and SIP pres)	Patient lived 2 months to be able to get 2 month interview, and from this interview there were no signs of moderate to severe functional disability	1=no (M2 and SIP pres)
sfdm2_adl>=4 (>=5 if sur)	Patient was unable to do 4 or more activities of daily living at month 2 after study entry. If the patient was not interviewed but the patient's surrogate was, the cutoff for disability was ADL	1= adl>=4 (>=5 if sur)
avtisst	Average TISS, Days 3-25	Days
dzgroup_Lung Cancer	The current group is lung cancer	1=Lung Cancer
sfdm2_SIP>=30	Sickness Impact Profile total score at 2 months	1=SIP>=30

Here, for more details of SUPPORT, it can be found in the links <https://hbiostat.org/data/repo/Csupport2.html> and <https://biostat.app.vumc.org/wiki/Main/SupportDesc>

References

395 References

- [1] D. R. Cox, Regression models and life-tables, *Journal of the Royal Statistical Society: Series B (Methodological)* 34 (2) (1972) 187–202.
- [2] J. L. Katzman, U. Shaham, A. Cloninger, J. Bates, T. Jiang, Y. Kluger, DeepSurv: personalized treatment recommender system using a Cox proportional hazards deep neural network, *BMC Medical Research Methodology* 18 (1) (2018) 1–12.
- [3] T. Ching, X. Zhu, L. X. Garmire, Cox-nnet: An artificial neural network method for prognosis prediction of high-throughput omics data, *PLoS computational biology* 14 (4) (2018) e1006076.
- 405 [4] J. Hao, Y. Kim, T.-K. Kim, M. Kang, PASNet: pathway-associated sparse deep neural network for prognosis prediction from high-throughput data, *BMC Bioinformatics* 19 (1) (2018) 1–13.
- [5] D. Gunning, D. W. Aha, DARPA’s explainable artificial intelligence (XAI) program, *AI Magazine* 40 (2) (2019) 44–58.
- 410 [6] D. W. Hosmer, S. Lemeshow, S. May, *Applied Survival Analysis: Regression Modeling of Time-to-Event Data*, 2nd Edition, 2008.
- [7] J. Fan, Y. Feng, Y. Wu, High-dimensional variable selection for Cox’s proportional hazards model, *Borrowing Strength: Theory Powering Applications – A Festschrift for Lawrence D. Brown* 6 (2010) 70–86.
- 415 [8] E. L. Kaplan, P. Meier, Nonparametric estimation from incomplete observations, *Journal of the American Statistical Association* 53 (282) (1958) 457–481.
- [9] N. Mantel, Evaluation of survival data and two new rank order statistics arising in its consideration, *Cancer Chemotherapy Reports* 50 (3) (1966) 163–170.
- 420

- [10] R. Peto, J. Peto, Asymptotically efficient rank invariant test procedures, *Journal of the Royal Statistical Society. Series A (General)* 135 (2) (1972) 185–207.
- [11] B. K. Natarajan, Sparse approximate solutions to linear systems, *SIAM Journal on Computing* 24 (2) (1995) 227–234.
- [12] J. Weston, A. Elisseeff, B. Schrölkopf, M. Tipping, Use of the zero norm with linear models and kernel methods, *The Journal of Machine Learning Research* 3 (2003) 1439–1461.
- [13] Y. Hamo, S. Markovitch, The COMPSET algorithm for subset selection, in: *IJCAI*, 2005.
- [14] R. Tibshirani, Regression shrinkage and selection via the Lasso, *Journal of the Royal Statistical Society: Series B (Methodological)* 58 (1) (1996) 267–288.
- [15] S. S. Chen, D. L. Donoho, M. A. Saunders, Atomic decomposition for basis pursuit, *Society for Industrial and Applied Mathematics Journal on Scientific Computing* 20 (1) (1998) 33–61.
- [16] J. Fan, R. Li, Variable selection via nonconcave penalized likelihood and its oracle properties, *Journal of the American statistical Association* 96 (456) (2001) 1348–1360.
- [17] J. Fan, W. Gong, Q. Sun, A provable two-stage algorithm for penalized hazards regression, *arXiv preprint arXiv:2107.02730v1*.
- [18] C. Wen, A. Zhang, S. Quan, X. Wang, BeSS: An R package for best subset selection in linear, logistic and Cox proportional hazards models, *Journal of Statistical Software* 94 (4) (2020) 1–24.
- [19] X. Wu, Q. Cheng, Algorithmic stability and generalization of an unsupervised feature selection algorithm, in: *NeurIPS*, 2021.

- [20] X. Wu, Q. Cheng, Fractal autoencoders for feature selection, in: AAAI, 2021.
- [21] F. E. Harrell, R. M. Califf, D. B. Pryor, K. L. Lee, R. A. Rosati, Evaluating
450 the yield of medical tests, *Journal of the American Medical Association*
247 (18) (1982) 2543–2546.
- [22] H. Steck, B. Krishnapuram, C. Dehing-oberije, P. Lambin, V. C. Raykar,
On ranking in survival analysis: Bounds on the concordance index, in:
NIPS, 2007.
- 455 [23] E. Graf, C. Schmoor, W. Sauerbrei, M. Schumacher, Assessment and com-
parison of prognostic classification schemes for survival data, *Statistics in*
Medicine 18 (17-18) (1999) 2529–2545.
- [24] G. W. Brier, Verification of forecasts expressed in terms of probability,
Monthly Weather Review 78 (1) (1950) 1–3.
- 460 [25] X. Glorot, Y. Bengio, Understanding the difficulty of training deep feed-
forward neural networks, in: AISTATS, 2010.
- [26] D. P. Kingma, J. L. Ba, Adam: A method for stochastic optimization, in:
ICLR, 2015.
- [27] *Probability and Stochastics*, 1st Edition, Erhan Çinlar, 2011.
- 465 [28] Y. Nesterov, *Lectures on Convex Optimization*, 2nd Edition, 2018.
- [29] J. Li, K. Cheng, S. Wang, F. Morstatter, R. P. Trevino, J. Tang, H. Liu,
Feature selection: a data perspective, *ACM Computing Surveys* 50 (6)
(2017) 1–45.
- [30] S. Pölsterl, Survival analysis for deep learning, in: [https://k-d-
470 w.org/blog/2019/07/survival-analysis-for-deep-learning/](https://k-d-w.org/blog/2019/07/survival-analysis-for-deep-learning/), 2019.
- [31] M. Goldstein, X. Han, A. Puli, A. J. Perotte, R. Ranganath, X-CAL: Ex-
plicit calibration for survival analysis, in: NeurIPS, 2020.

- [32] L. Manduchi, R. Marcinkevičs, M. C. Massi, T. Weikert, A. Sauter, V. Gotta, T. Müller, F. Vasella, M. C. Neidert, M. Pfister, B. Stieltjes, J. E. Vogt, A deep variational approach to clustering survival data, in: 475 ICLR, 2022.
- [33] C. Desmedt, F. Piette, S. Loi, Y. Wang, F. Lallemand, B. Haibe-Kains, G. Viale, M. Delorenzi, Y. Zhang, M. S. d’Assignies, J. Bergh, R. Lidereau, P. Ellis, A. L. Harris, J. G. Klijn, J. A. Foekens, F. Cardoso, M. J. Piccart, 480 M. Buyse, C. Sotiriou, on behalf of the TRANSBIG Consortium, Strong time dependence of the 76-gene prognostic signature for node-negative breast cancer patients in the TRANSBIG multicenter independent validation series, *Clinical Cancer Research* 13 (11) (2007) 3207–3214.
- [34] M. Schmid, M. N. Wright, A. Ziegler, On the use of Harrell’s C for clinical 485 risk prediction via random survival forests, *Expert Systems with Applications* 63 (2016) 450–459.
- [35] J. M. Bland, D. G. Altman, The logrank test, *British Medical Journal* 328 (7447) (2004) 1073.
- [36] W. A. Knaus, F. E. Harrell, J. Lynn, L. Goldman, R. S. Phillips, A. F. Connors, N. V. Dawson, W. J. Fulkerson, R. M. Califf, N. Desbiens, P. Layde, 490 R. K. Oye, P. E. Bellamy, R. B. Hakim, D. P. Wagner, The SUPPORT prognostic model: Objective estimates of survival for seriously ill hospitalized adults, *Annals of Internal Medicine* 122 (3) (1995) 191–203.
- [37] C.-H. Yip, A. Rhodes, Estrogen and progesterone receptors in breast cancer, 495 *Future oncology* 10 (14) (2014) 2293–2301.
- [38] A. M. Farcas, S. Nagarajan, S. Cosulich, J. S. Carroll, Genome-wide estrogen receptor activity in breast cancer, *Endocrinology* 16 (2) (2021) bqaa224.
- [39] F. Hanif, K. Muzaffar, K. Perveen, S. M. Malhi, S. U. Simjee, Glioblastoma multiforme: A review of its epidemiology and pathogenesis through clinical

- 500 presentation and treatment, *Asian Pacific Journal of Cancer Prevention* 18 (1) (2017) 3–9.
- [40] S. Bozdag, A. Li, G. Riddick, Y. Kotliarov, M. Baysan, F. M. Iwamoto, M. C. Cam, S. Kotliarova, H. A. Fine, Age-specific signatures of glioblastoma at the genomic, genetic, and epigenetic levels, *PLOS ONE* 8 (4) (2013) e62982.
- 505 [41] J. Lu, M. C. Cowperthwaite, M. G. Burnett, M. Shpak, Molecular predictors of long-term survival in glioblastoma multiforme patients, *PLOS ONE* 11 (4) (2016) e0154313.
- [42] A. Yoshino, A. Ogino, K. Yachi, T. Ohta, T. Fukushima, T. Watanabe, Y. Katayama, Y. Okamoto, N. Naruse, E. Sano, K. Tsumoto, Gene expression profiling predicts response to temozolomide in malignant gliomas, *International Journal of Oncology* 36 (6) (2010) 1367–1377.
- 510 [43] N. K. Gerber, A. Goenka, S. Turcan, M. Reyngold, V. Makarov, K. Kannan, K. Beal, A. Omuro, Y. Yamada, P. Gutin, C. W. Brennan, J. T. Huse, T. A. Chan, Transcriptional diversity of long-term glioblastoma survivors, *Neuro-Oncology* 16 (9) (2014) 1186–1195.
- [44] E. H. Panosyan, H. J. Lin, J. Koster, J. L. L. III, In search of druggable targets for GBM amino acid metabolism, *BMC Cancer* 17 (1) (2017) 1–12.